DOI: https://doi.org/10.15407/pmach2019.03.026

UDC 539.3

CHAOTIC OSCILLATIONS OF A KINEMATICALLY EXCITED FLAT SHELL DURING GEOMETRICALLY NON-LINEAR DEFORMATION

Konstantin V. Avramov
kvavramov@gmail.com
ORCID: 0000-0002-8740-693X

Kseniya F. Cheshko
cheshko.ks@gmail.com
ORCID: 0000-0001-8662-4209

Oleg F. Polishchuk
PolischukOleg@nas.gov.ua
ORCID: 0000-0003-1266-9847

A. Podgorny Institute of Mechanical Engineering Problems of NASU,
2/10, Pozharskyi Str.,
Kharkiv, 61046, Ukraine

We study the forced oscillations of a cantilevered flat shell of constant curvature. These movements are excited by a kinematic periodic embedding motion. To describe geometrically non-linear deformation, the non-linear theory of Donel shells is used. To build a non-linear dynamic system with a finite number of degrees of freedom, the method of specified forms is used. Since the eigen frequencies of longitudinal and torsional oscillations are much higher than bending ones, the inertial forces in the longitudinal and torsional directions are not taken into account. Therefore, the generalized coordinates of longitudinal and torsional oscillations are expressed in terms of bending ones. As a result, a non-linear dynamic system with respect to bending generalized coordinates is obtained. To calculate the eigen forms of linear oscillations, by using which the non-linear dynamic problem decomposes, the Rayleigh-Ritz method is used. Then only kinematic boundary conditions are satisfied. When the solution converges, the force boundary conditions are automatically satisfied. To study the convergence of eigen frequencies, calculations were performed with a different number of basis functions, which are B-splines. A comparison is made with the experimental data on the analysis of eigen frequencies, with the data published in authors' previous article. To numerically analyze the non-linear periodic oscillations, a two-point boundary value problem is solved for ordinary differential equations by the shooting method. The stability of periodic motions and their bifurcations are estimated using multipliers. To study the bifurcations of periodic oscillations, the parameter continuation method is applied. In the region of the main resonance, saddle-node bifurcations, period-doubling bifurcations, and Neimark-Sacker bifurcations are found. To study the steady-state almost periodic and chaotic oscillations, Poincaré sections, spectra of Lyapunov characteristic exponents, and spectral densities are calculated, with the stroboscopic phase portrait used as Poincaré sections. The properties of steady-state oscillations are investigated with a quasistatic change in the frequency of the disturbing action.

Keywords: *non-linear periodic oscillations of a flat shell, stability of oscillations, almost periodic oscillations, chaotic oscillations.*

Introduction

Shell designs are widely used in aerospace engineering, power engineering, mechanical engineering, construction, and nanotechnology. These structures have high rigidity with a relatively small mass, which is important for engineers. A lot of research is devoted to the oscillations of such structures. A detailed review of the work carried out in this area is presented in [1–3].

In this article, a non-linear model of the forced oscillations of a kinematically excited flat shell during geometrically non-linear deformation is constructed. To study resonant forced oscillations, a numerical approach is developed. The approach includes a solution to the two-point boundary value problem for non-linear ordinary differential equations and a method of continuation of solutions. With this approach, the bifurcation behavior of resonant oscillations is investigated, as well as saddle-nodal bifurcations, period-doubling bifurcations, and Neymark-Sacker bifurcations are discovered. It is shown that, as a result of some of these bifurcations, chaotic oscillations are formed, which are studied numerically. Order-chaos transitions are discovered.

Problem Statement and Basis Equations

We investigate the forced oscillations of a cantilever cylindrical panel (flat shell) (Fig. 1). The radius of curvature of the shell middle surface is constant. We associate the shell with a curvilinear coordinate system x, θ, z. The axis x is directed along the generating shell perpendicular to its embedment; the axis θ is directed in the circumferential direction of the shell; the axis z is perpendicular to the middle surface of the shell. The side

$x = 0$ is clamped, and all the other sides are free. The forced oscillations of the shell are excited by a kinematic embedding motion. The clamped side moves like this:

$$\eta(t) = \eta_0 \cos \omega t, \quad (1)$$

where η_0 is the amplitude of embedment oscillations, ω is the frequency of these oscillations. We denote the projections of middle surface displacements along the x, θ, z axes by $u(x, \theta, t)$, $v(x, \theta, t)$, $w(x, \theta, t)$. These displacement projections are the main unknowns of the problem. If the amplitude of the kinematic excitation of the embedment η_0 is small, then the oscillations of the shell will be linear.

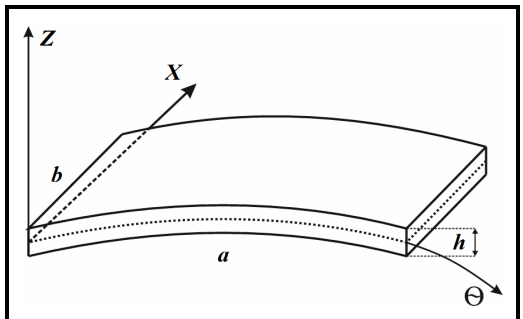

Fig. 1. Flat shell

If we increase η_0, we can achieve such a value of this parameter that the radial displacements w (x, θ, t) are comparable with the shell thickness h. Then a geometrically non-linear deformation will be observed. In this case, the deformations are small, and the movements are moderate. Since the deformations are small, then the components of stress and strain tensors satisfy Hooke's law.

To describe geometrically non-linear deformation, we use the non-linear theory of Donella shells [3]

$$\varepsilon_{11} = \frac{\partial u}{\partial \theta} + \frac{w}{R} + \frac{1}{2}\left(\frac{\partial w}{\partial \theta}\right)^2; \quad \varepsilon_{22} = \frac{\partial v}{\partial x} + \frac{1}{2}\left(\frac{\partial w}{\partial x}\right)^2; \quad \varepsilon_{12} = \frac{\partial u}{\partial x} + \frac{\partial v}{\partial \theta} + \frac{\partial w}{\partial \theta}\frac{\partial w}{\partial x}; \quad (2)$$

$$k_1 = \frac{-\partial^2 w}{\partial \theta^2}; \quad k_2 = \frac{-\partial^2 w}{\partial x^2}; \quad k_3 = \frac{-\partial^2 w}{\partial \theta \partial x},$$

where $\varepsilon_{11}, \varepsilon_{22}, \varepsilon_{12}$ are the elements of the strain tensor of the shell middle surface; k_1, k_2, k_3 are the changes in the middle surface curvature. The potential energy of the shell is represented as [3]:

$$\Pi = \frac{Eh}{2(1-\mu^2)} \int_0^a \int_0^b \left\{ \varepsilon_{11}^2 + \varepsilon_{22}^2 + 2\mu\varepsilon_{11}\varepsilon_{22} + \frac{1-\mu}{2}\varepsilon_{12}^2 \right\} d\theta dx + \frac{D}{2} \int_0^a \int_0^b \left\{ k_1^2 + k_2^2 + 2\mu k_1 k_2 + \frac{1-\mu}{2} k_3^2 \right\} d\theta dx + \quad (3)$$

$$+ \frac{D}{R} \int_0^a \int_0^b \left\{ \varepsilon_{11} k_1 + \varepsilon_{22} k_2 + \mu\varepsilon_{11} k_2 + \mu\varepsilon_{22} k_1 + \frac{1-\mu}{2}\varepsilon_{12} k_3 \right\} d\theta dx,$$

where $D = \frac{Eh}{2(1-\mu^2)}$; E, μ – are Young's modulus and Poisson's ratio; a, b are the side lengths of the flat shell.

We write the kinetic energy of the shell in the form

$$T = \frac{\rho h}{2} \int_0^a \int_0^b \left((\dot{w} + \dot{\eta})^2 + \dot{u}^2 + \dot{v}^2 \right) d\theta dx, \quad (4)$$

where ρ is the density of the shell material.

To find the eigen frequencies and forms of the linear oscillations of the shell, we will use the Rayleigh-Ritz method, which requires satisfying only the kinematic boundary conditions. In this case, when the solution converges, the force boundary conditions are automatically satisfied [2]. When the Rayleigh-Ritz method is used, on the three free sides, only the ignorable force boundary conditions are set. The geometric boundary conditions on the clamped side of the shell take the following form:

$$w\big|_{x=0} = 0; \quad \left.\frac{\partial w}{\partial x}\right|_{x=0} = 0; \quad u\big|_{x=0} = 0; \quad v\big|_{x=0} = 0. \quad (5)$$

Model of Non-linear Oscillations

Consider the shell oscillations during geometrically non-linear deformation. Then the projections of displacements can be represented as expansions in their eigenforms of oscillations as follows:

$$w(x,\theta,t)=\sum_{k=1}^{N_1}\xi_k(t)W_k(x,\theta);\ u(x,\theta,t)=\sum_{k=1}^{N_2}\xi_{k+N_1}(t)U_k(x,\theta);\ v(x,\theta,t)=\sum_{k=1}^{N_3}\xi_{k+N_1+N_2}(t)V_k(x,\theta), \tag{6}$$

where $N_* = N_1 + N_2 + N_3$ is the number of degrees of freedom of the structure; $\xi = [\xi_1, ..., \xi_{N_*}]$ is the vector of the generalized coordinates of the structure; (W_k, U_k, V_k) is the eigenform of linear oscillations. To calculate the eigenforms of linear oscillations, the Rayleigh-Ritz method is used. Therefore, with a good approximation of solutions, the eigenforms included in expansion (6) satisfy both geometric and force boundary conditions. Decompositions (6) are introduced into kinetic energy (4). As a result, with (2) taken into account, the kinetic energy takes a quadratic form with respect to generalized velocities and $\dot{\eta}$ in the form (1): $T = T(\dot{\xi}_1, ..., \dot{\xi}_{N_*}, \dot{\eta})$. We will introduce decompositions (6) into potential energy (3). Then the potential energy contains quadratic, cubic, and fourth-degree terms with respect to the generalized coordinates. The potential energy is represented as: $\prod = \prod(\xi_1, ..., \xi_N)$. Now we work out the Lagrange equations of motion for the construction. In matrix form, these equations will take the following form:

$$\begin{gathered}\mathbf{M}^{(1)}\ddot{\mathbf{q}}^{(w)}+\mathbf{C}^{(1,1)}\mathbf{q}^{(w)}+\mathbf{C}^{(1,2)}\mathbf{q}^{(u)}+\mathbf{C}^{(1,3)}\mathbf{q}^{(v)}+\mathbf{C}^{(1,4)}(\mathbf{q}(\mathbf{w}))\mathbf{q}^{(w)}+\mathbf{C}^{(1,5)}(\mathbf{q}(\mathbf{u}))\mathbf{q}^{(w)}+\mathbf{C}^{(1,6)}(\mathbf{q}(\mathbf{v}))\mathbf{q}^{(w)}+\\ +\mathbf{C}^{(1,7)}(\mathbf{q}(\mathbf{w}),\mathbf{q}^{(w)})\mathbf{q}^{(w)}+\mathbf{F}^{(1)}\ddot{\eta}=\mathbf{0},\\ \mathbf{M}^{(2)}\ddot{\mathbf{q}}^{(u)}+\mathbf{C}^{(2,1)}\mathbf{q}^{(w)}+\mathbf{C}^{(2,2)}\mathbf{q}^{(u)}+\mathbf{C}^{(2,3)}\mathbf{q}^{(v)}+\mathbf{C}^{(2,4)}(\mathbf{q}(\mathbf{w}))\mathbf{q}^{(w)}=\mathbf{0},\\ \mathbf{M}^{(3)}\ddot{\mathbf{q}}^{(v)}+\mathbf{C}^{(3,1)}\mathbf{q}^{(w)}+\mathbf{C}^{(3,2)}\mathbf{q}^{(u)}+\mathbf{C}^{(3,3)}\mathbf{q}^{(v)}+\mathbf{C}^{(3,4)}(\mathbf{q}(\mathbf{w}))\mathbf{q}^{(w)}=\mathbf{0},\end{gathered} \tag{7}$$

where $q^{(w)} = (\xi_1, ..., \xi_{N_1})^{\mathrm{T}}$, $q^{(u)} = (\xi_{N_1+1}, ..., \xi_{N_1+N_2})^{\mathrm{T}}$, $q^{(v)} = (\xi_{N_1+N_2+1}, ..., \xi_{N_1})^{\mathrm{T}}$; $\boldsymbol{C}^{(1,1)}$, $\boldsymbol{C}^{(1,2)}$, $\boldsymbol{C}^{(1,3)}$, $\boldsymbol{C}^{(2,1)}$, $\boldsymbol{C}^{(2,2)}$, $\boldsymbol{C}^{(2,3)}$, $\boldsymbol{C}^{(3,1)}$, $\boldsymbol{C}^{(3,2)}$, $\boldsymbol{C}^{(3,3)}$ are the submatrices of structural rigidity; $\boldsymbol{M}^{(1)}$, $\boldsymbol{M}^{(2)}$, $\boldsymbol{M}^{(3)}$ are the submatrices of the mass of the structure; $\mathbf{C}^{(1,4)}(\mathbf{q}(\mathbf{w})), \mathbf{C}^{(1,5)}(\mathbf{q}(\mathbf{u})), \mathbf{C}^{(1,6)}(\mathbf{q}(\mathbf{v})), \mathbf{C}^{(2,4)}(\mathbf{q}(\mathbf{w})), \mathbf{C}^{(3,4)}(\mathbf{q}(\mathbf{w}))$ are the matrix functions whose elements are the linear functions of the corresponding generalized coordinates; $\mathbf{C}^{(1,7)}(\mathbf{q}(\mathbf{w}),\mathbf{q}^{(w)})$ is the matrix function whose elements are the quadratic form of the generalized coordinates.

For thin shells, the frequencies of longitudinal and torsional oscillations are much higher than those of bending ones. Therefore, in the second and third matrix equations of system (7), we neglect the inertial terms. Then the second and third matrix equations of system (7) can be rewritten as:

$$\mathbf{q}^{(u)}=\boldsymbol{\alpha}^{(1)}\mathbf{q}^{(w)}+\boldsymbol{\beta}^{(1)}(\mathbf{q}^{(w)})\mathbf{q}^{(w)};\quad \mathbf{q}^{(v)}=\boldsymbol{\alpha}^{(2)}\mathbf{q}^{(w)}+\boldsymbol{\beta}^{(2)}(\mathbf{q}^{(w)})\mathbf{q}^{(w)}, \tag{8}$$

where $\boldsymbol{\alpha}^{(1)}, \boldsymbol{\alpha}^{(2)}$ are constant matrices; $\boldsymbol{\beta}^{(1)}(\mathbf{q}^{(w)}), \boldsymbol{\beta}^{(2)}(\mathbf{q}^{(w)})$ are the matrices whose elements are the linear functions of the generalized coordinates. Equation (8) is introduced into the first matrix equation of system (7). Then, as a result, we get

$$\mathbf{M}^{(1)}\ddot{\mathbf{q}}^{(w)}+\mathbf{R}\dot{\mathbf{q}}^{(w)}+\mathbf{K}^{(1)}\mathbf{q}^{(w)}+\mathbf{K}^{(2)}(\mathbf{q}^{(w)})\mathbf{q}^{(w)}+\mathbf{K}^{(3)}(\mathbf{q}^{(w)},\mathbf{q}^{(w)})\mathbf{q}^{(w)}+\mathbf{F}^{(1)}\ddot{\eta}=\mathbf{0}, \tag{9}$$

where $\mathbf{M}^{(1)}, \mathbf{R}, \mathbf{K}^{(1)}$ are constant matrices; $\mathbf{K}^{(2)}(\mathbf{q}^{(w)})$ is the matrix whose elements are the linear functions of the generalized coordinates.

In the future, we will introduce a vector of dimensionless variables and parameters

$$\mathbf{y} = (y_1, ..., y_{N_1});\quad y_i = \frac{\xi_i}{h};\quad i = 1, ..., N_1;\quad \tau = \omega_1 t, \tag{10}$$

where ω_1 is the first eigen frequency of linear oscillations. Dynamic system (9) with respect to dimensionless variables and parameters (10) will take the following form:

$$\hat{\mathbf{M}}^{(1)}\mathbf{y}'' + \hat{\mathbf{R}}\mathbf{y}' + \hat{\mathbf{K}}^{(1)}\mathbf{y} + \hat{\mathbf{K}}^{(2)}(\mathbf{y})\mathbf{y} + \hat{\mathbf{K}}^{(3)}(\mathbf{y},\mathbf{y})\mathbf{y} = \hat{\mathbf{F}}^{(1)}\hat{\eta}_0\hat{\omega}^2\cos(\hat{\omega}\tau), \tag{11}$$

where $\mathbf{M}^{(1)} = m\hat{\mathbf{M}}^{(1)}$; $\hat{\mathbf{R}} = \frac{1}{m\omega_1}\mathbf{R}$; $\hat{\mathbf{K}}^{(1)} = \frac{1}{m\omega_1^2}\mathbf{K}^{(1)}$; $\hat{\mathbf{K}}^{(2)}(\mathbf{y}) = \frac{1}{m\omega_1^2}\mathbf{K}^{(2)}(\mathbf{q}^{(w)})$; $\hat{\mathbf{K}}^{(3)}(\mathbf{y},\mathbf{y}) = \frac{1}{m\omega_1^2}\mathbf{K}^{(3)}(\mathbf{q}^{(w)},\mathbf{q}^{(w)})$;

$\hat{\mathbf{F}}_1^{(1)} = \frac{1}{m}\mathbf{F}_1^{(1)}$; $\hat{\omega} = \frac{\omega}{\omega_1}$; $\hat{\eta}_0 = \frac{\eta_0}{h}$; m is the shell mass.

Suppose that periodic oscillations are found in system (11), which are represented as: $\mathbf{y}(t) = \mathbf{y}(\tau + T)$, where $T = \frac{2\pi}{\omega}$ is the oscillation period. We study the stability of the periodic motions found. To analyze the stability of periodic oscillations, we rewrite dynamic system (9) with respect to the phase coordinates $\mathbf{p} = (\mathbf{y}, \dot{\mathbf{y}})$ in vector form as follows:

$$\dot{\mathbf{p}} = \mathbf{f}(\mathbf{p}, \mathbf{t}). \tag{12}$$

Now, near the periodic motion $\mathbf{p}_*(\mathrm{t}) = (\mathbf{p}_*; \dot{\mathbf{p}}_*)$, we introduce a vector of small perturbations $\xi(t)$. Then the vector $\xi(t)$ satisfies the following system of equations in variations [4]:

$$\dot{\xi} = \mathbf{Df}(\mathbf{p}_*(t), t)\xi, \tag{13}$$

where $\mathbf{Df}(\mathbf{p}_*(t), t)$ is the Jacobi matrix of the vector function $\mathbf{f}(\mathbf{p}_*(t), t)$. From the solutions to equations (13), a quadratic fundamental matrix $\mathbf{\Phi}(t)$ is constructed. This matrix satisfies the following matrix initial condition: $\mathbf{\Phi}(t) = \mathbf{E}$, where $\mathbf{E}$ is the identity matrix. The matrix $\mathbf{\Phi}(T)$ is called a monodromy matrix, and its eigenvalues are called multipliers ρ [4]

$$Det[\mathbf{\Phi}(T) - \rho\mathbf{E}] = 0.$$

Using the multiplier values, we estimate the stability of a periodic motion and its bifurcation.

When constructing non-linear dynamical system (9), we use the eigenforms of linear oscillations, which are represented in decomposition (6). To calculate them, the Rayleigh-Ritz method [5] is used. We represent the linear oscillations of the shell in the form

$$u = U(x,\theta)\cos(\omega t); \quad v = V(x,\theta)\cos(\omega t); \quad w = W(x,\theta)\cos(\omega t), \tag{14}$$

where $U(x,\theta), V(x,\theta), W(x,\theta)$ are the functions to be defined. They are decomposed into basis functions as follows:

$$W(x,\theta) = \sum_{k=1}^{N_1} A_k w_k(x,\theta); \quad U(x,\theta) = \sum_{k=1}^{N_2} A_{k+N_1} u_k(x,\theta); \quad V(x,\theta) = \sum_{k=1}^{N_3} A_{k+N_1+N_2} v_k(x,\theta), \tag{15}$$

where $u_k(x,\theta), v_k(x,\theta), w_k(x,\theta)$ are the basis functions satisfying geometric boundary conditions (5); $A_1, ..., A_N$ are the constants to be calculated; $N = N_1 + N_2 + N_3$. Decompositions (15) are introduced in (14). B-splines are used as basis functions [6, 7]. The effectiveness of this approach is shown in [6]. Then decomposition (15) can be represented as

$$W(x,\theta) = \sum_{k_1=1}^{M_1+3}\sum_{k_2=1}^{M_2+3} a_{k_1k_2}^{(w)} \overline{w}_{k_1k_2}(x,\theta); \; U(x,\theta) = \sum_{k_1=1}^{M_1+3}\sum_{k_2=1}^{M_2+3} a_{k_1k_2}^{(u)} \overline{u}_{k_1k_2}(x,\theta); \; V(x,\theta) = \sum_{k_1=1}^{M_1+3}\sum_{k_2=1}^{M_2+3} a_{k_1k_2}^{(v)} \overline{v}_{k_1k_2}(x,\theta). \tag{16}$$

where $\overline{w}_{k_1k_2}(x,\theta) = x^2 B_3\left(\frac{M_1\theta}{a} + k_1 - 2\right) B_3\left(\frac{M_2 x}{b} + k_2 - 2\right)$;

$\overline{u}_{k_1k_2}(x,\theta) = \overline{v}_{k_1k_2}(x,\theta) = xB_3\left(\frac{M_1\theta}{a} + k_1 - 2\right) B_3\left(\frac{M_2 x}{b} + k_2 - 2\right)$;

$$B_3(\phi)=\begin{cases} 0, \left|-\infty < \phi \le -2 \right. \\ 0.25(\phi+2)^3, \left|-2 < \phi \le -1 \right. \\ -0.75\phi^3 - 1.5\phi^2 + 1, \left|-1 < \phi \le 0 \right. \\ 0.75\phi^3 - 1.5\phi^2 + 1, \left|0 < \phi \le 1 \right. \\ -0.25\phi^3 + 1.5\phi^2 - 3\phi + 2 \left|1 < \phi \le 2 \right. \\ 0, \left|2 < \phi \le \infty \right. \end{cases},$$

M_1+3 is the number of splines in the θ direction; M_2+3 is the number of splines in the x direction; $B_3(\phi)$ is the third order Schönberg spline. We represent the unknown parameters of decomposition (16) as $a=\left(a_{1,1}^{(w)},...,a_{M_1+3,M_2+3}^{(w)},a_{1,1}^{(u)},...,a_{1,1}^{(v)},...\right)=(a_1,...,a_N)$. These parameters describe the forms of eigen oscillations, which are found from the eigenvalue problem $\left(K-\omega^2 M\right)a^{\mathrm{T}}=0$, where K, M are the mass and stiffness matrices.

Numerical Analysis of Forced Periodic Oscillations

We study the shell made of grade 10 steel. The shell parameters were taken as follows: E=2,06·10^{11} Pa; ρ=7,856·10^3 kg/м^3; a=0,2 m; b=0,24 m; μ=0,3; h=3·10^{-3} m; R=0,26 m.

The linear oscillations of this shell were studied experimentally. The methodology of the experiment and the results of the analysis of the linear oscillations are presented in article [8].

To study the oscillations of the flat shell, we use the Rayleigh-Ritz method. Consider the convergence of eigen frequencies. To do this, we will perform calculations for a different number of basis functions in decomposition (15). The results of the analysis of the eigen frequencies are presented in Table 1. The heading of the table shows the number of terms in decomposition (15), for which the eigen frequencies were calculated. The numbers of the first ten eigen frequencies are given in the first column. In the second, third, and fourth ones, the eigen frequencies are shown at $N_1=N_2=N_3=5$; $N_1=N_2=N_3=7$ and $N_1=N_2=N_3=8$, respectively. The calculation results obtained by using the ANSYS software package are presented in the fifth column of the table. So, there is a convergence of the results obtained, that is, the results obtained by the Rayleigh-Ritz method and the data obtained by using the ANSYS software package are close. The sixth column of the table shows the first five eigen frequencies obtained experimentally, the seventh one, the relative difference of the eigen frequencies, δ, obtained both experimentally and by using the ANSYS software package. The relative difference of the eigen frequencies, δ, is valid.

Table 1. Eigen frequencies of shell oscillations

Eigen frequencies	N_1=N_2=N_3=5	N_1=N_2=N_3=7	N_1=N_2=N_3=8	ANSYS	Experiment	δ
ω_1, Hz	154.76	152.83	152.76	152.38	140.00	0.08
ω_2, Hz	246.47	242.67	242.56	246.49	231.00	0.06
ω_3, Hz	528.60	499.24	498.82	487.61	445.00	0.09
ω_4, Hz	624.48	602.42	600.93	600.76	545.00	0.1
ω_5, Hz	750.96	719.35	718.80	714.15	714.00	$2.1\cdot10^{-4}$
ω_6, Hz	1345.94	1209.47	1178.90	1153.30	–	–
ω_7, Hz	1386.65	1298.25	1287.23	1281.90	–	–
ω_8, Hz	1457.81	1303.60	1303.03	1295.60	–	–
ω_9, Hz	1728.89	1429.28	1428.60	1419.80	–	–
ω_{10}, Hz	2047.07	1659.62	1616.69	1584.30	–	–

As follows from Table 1, the shell under consideration is extremely rich in internal resonances that satisfy the following relations:

$$\frac{3\omega_1}{\omega_3}=0.91;\frac{2\omega_2}{\omega_3}=0.97;\frac{3\omega_2}{\omega_5}=1.01;\frac{2\omega_4}{\omega_6}=1.01;\frac{2\omega_4}{\omega_7}=0.93;\frac{2\omega_5}{\omega_9}=1.006;\frac{\omega_6}{\omega_7}=0.91;\frac{\omega_7}{\omega_8}=0.98;\frac{\omega_8}{\omega_9}=0.91$$

The internal resonances significantly affect the non-linear deformation of the structure [9].

Consider the non-linear oscillations of the flat cantilever shell under the conditions of the kinematic excitation of the embedment. In the numerical calculations of the non-linear oscillations, the amplitudes of the disturbing action were taken as follows: $\hat{\eta}_0 = 0{,}01$. The matrix $\hat{R}$ in (11) was reduced to the form: $\hat{R} = diag(\alpha,\alpha,...,\alpha)$; $\alpha = 0.01$. Later, the forced non-linear steady-state oscillations near the second fundamental resonance were studied numerically $\omega = \omega_2 + \alpha$, where α – is the detuning parameter, which is a small value. In decomposition (6), we take into account the first five eigen modes of oscillations.

To study the resonant periodic oscillations, two-point boundary value problem (12) was solved for a system of ordinary differential equations by the shooting method. To calculate the periodic oscillations in a wide range of the perturbation frequency, $\hat{\omega}$, we used the parameter continuation method. The combined use of the shooting method and the parameter continuation method to study periodic non-linear oscillations are presented in monograph [9]. To analyze the stability of periodic oscillations, multipliers were calculated.

In the numerical analysis of the steady-state oscillations near the second main resonance, it was found that the generalized coordinates y_1 and y_4 are passive coordinates, and have practically no effect on the system dynamics. The passive coordinates are understood as generalized coordinates with small amplitudes that have little effect on the system dynamics [9]. Therefore, the non-linear dynamics of the system with three degrees of freedom y_2, y_3, y_5 will be investigated further. The amplitude-frequency characteristic of resonant periodic oscillations is shown in Fig. 2. Here, the scale of the generalized coordinate y_2 is plotted along the ordinate axis, which is indicated by A, and the frequency of the disturbing action $\hat{\omega}$ is plotted along the abscissa. The solid line shows steady-state oscillations, while the dotted line shows unsteady ones.

Now consider the bifurcation behavior of periodic oscillations, which is shown in Fig. 2. Here are observed saddle-node bifurcations, period-doubling bifurcations, and Neymark-Sacker bifurcations, which are denoted by SN, PD and NS, respectively. The significance of these bifurcations for the occurrence of subharmonic, almost periodic, and chaotic oscillations are highlighted in monograph [9].

At the points of period-doubling bifurcations, second-order subharmonic oscillations arise. Such oscillations are indicated in Figure 3 by bold lines. The steady-state subharmonic oscillations are indicated by the solid line, and the unsteady ones, by the dashed line.

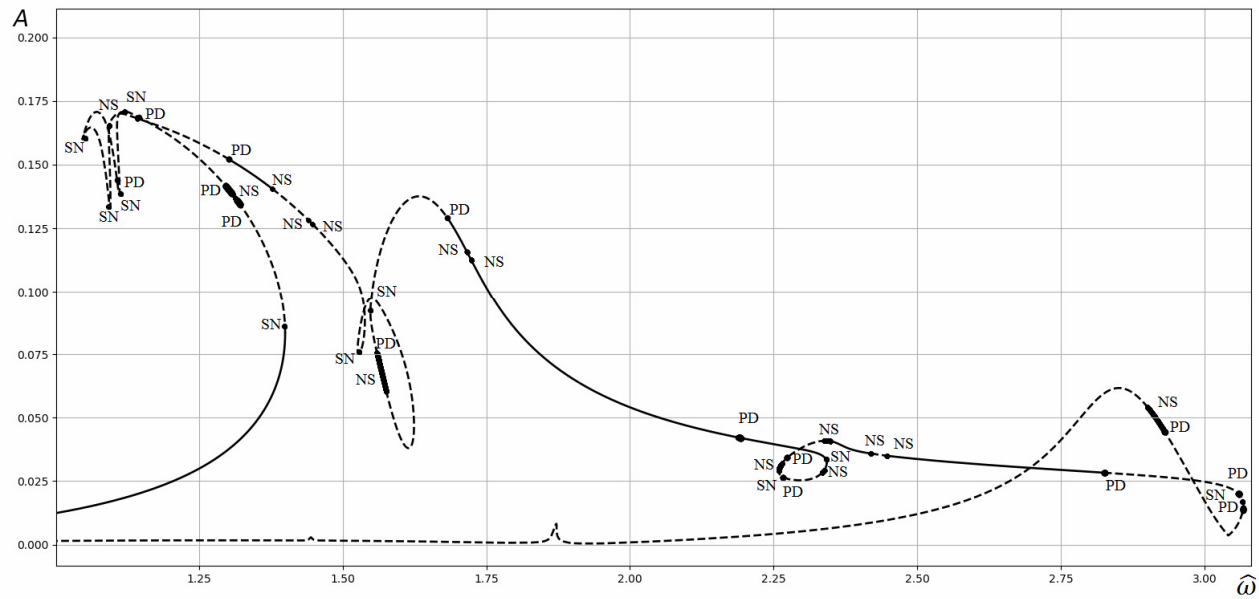

Fig. 2. Amplitude-frequency characteristic of resonant oscillations

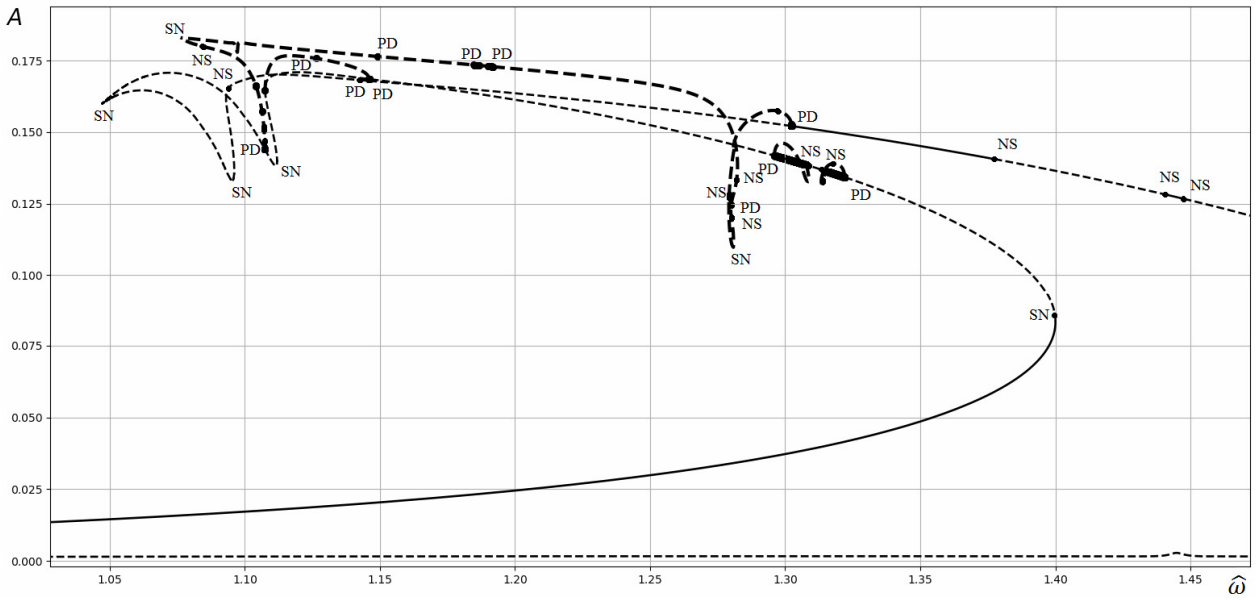

a

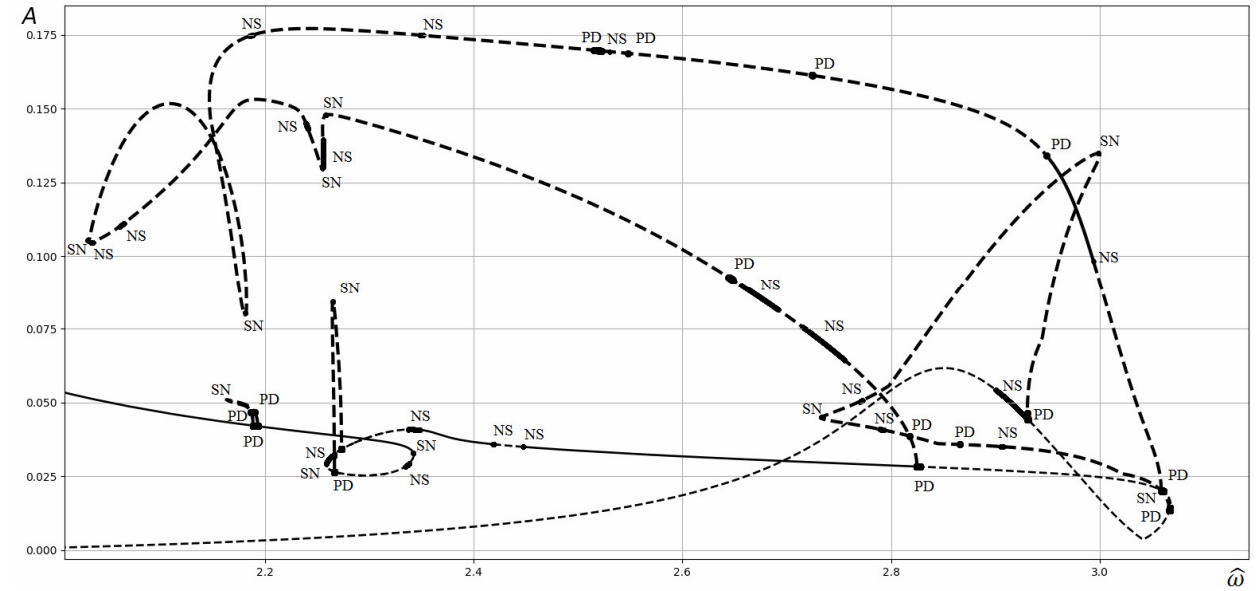

b

Fig. 3. Amplitude-frequency characteristic of subharmonic oscillations:
a – ω[1.0; 1.46]; b – ω[1.46; 3.1]

Numerical Simulation of Chaotic Oscillations

As follows from Fig. 2, in the region of the main resonance $\hat{\omega} \in [1.41; 1.72]$, there are no steady periodic oscillations. Therefore, in this frequency range we will investigate other types of steady-state motions. To do this, we integrate the system of equations (12) for different values of the frequency of the disturbing action $\hat{\omega}$ by the Runge-Kutta method with a variable pitch. As the initial conditions for the numerical integration, we use the initial conditions for non-steady-state periodic oscillations, which are shown in Fig. 2. The results of the numerical integration in the time interval $\tau \in [0; 1000T]$ are considered as a transition process, and are not taken into account in the analysis. Analyzed are the results of the numerical integration at $\tau > 1000T$.

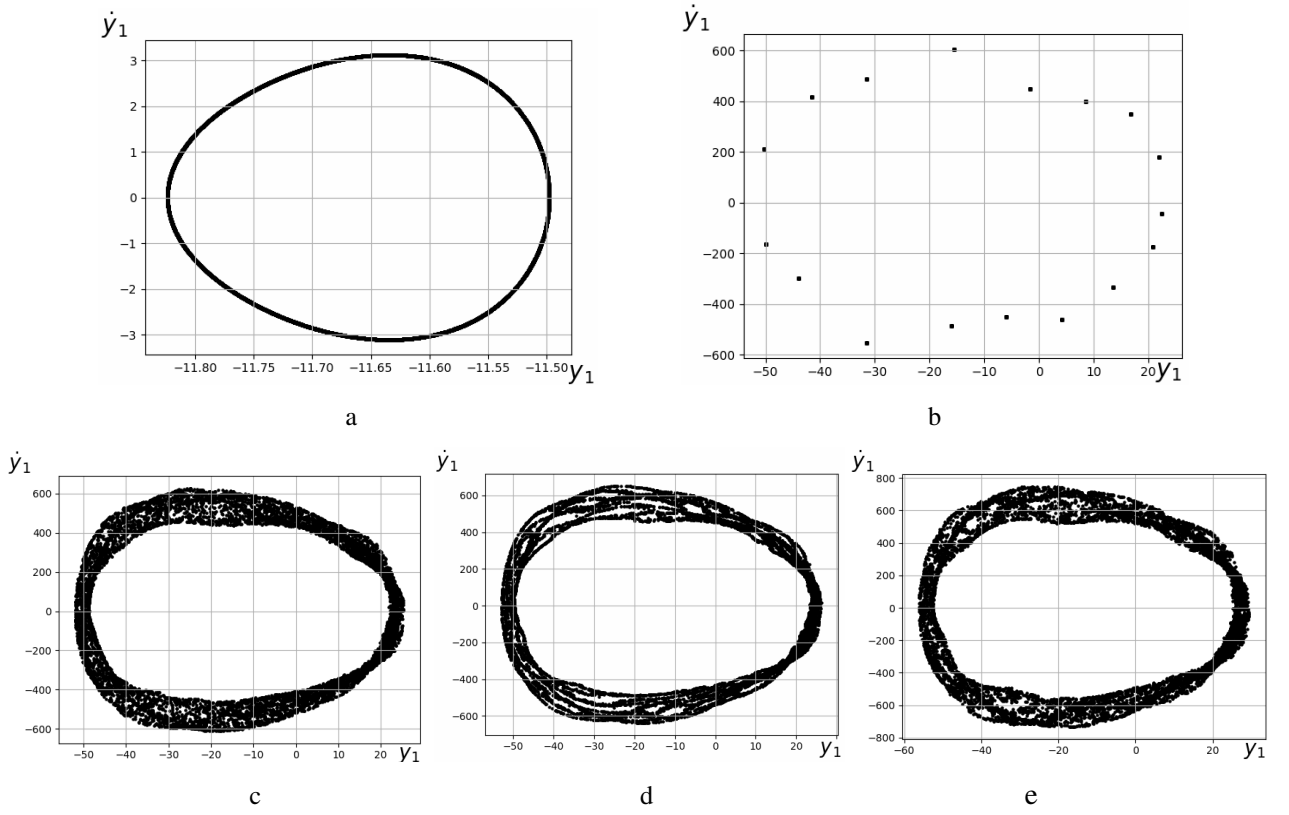

Fig.4. Poincaré sections of steady-state oscillations at the following frequencies of the disturbing action:
a – $\hat{\omega}$=1.38070; b – $\hat{\omega}$=1.4476; c – $\hat{\omega}$=1.4525; d – $\hat{\omega}$=1.50018; e – $\hat{\omega}$=1.66095

To study the steady-state oscillations, Poincaré sections, spectra of Lyapunov characteristic exponents, and spectral densities were analyzed, with the stroboscopic phase portrait used as Poincaré sections. The numerical methods for calculating the above three characteristics are covered in monograph [7].

The results of the calculation of the spectrum of Lyapunov characteristic indicators $\lambda_i; i = 1, 2, \ldots$ at different frequencies of the disturbing load are presented in Table 2. Now we study the properties of steady-state oscillations with a quasistatic change in the frequency of the disturbing action $\hat{\omega}$.

Table 2. Spectrum of characteristic Lyapunov indicators

ω	λ_1	λ_2	λ_3	λ_4
1.4476	$-4.1095\cdot10^{-2}$	$-5.9160\cdot10^{-2}$	$-5.9180\cdot10^{-2}$	-0.2110
1.4525	$1.0280\cdot10^{-2}$	$-5.8000\cdot10^{-2}$	$-3.2750\cdot10^{-2}$	-0.1560
1.4727	$2.8590\cdot10^{-2}$	$-7.0614\cdot10^{-2}$	$-7.5651\cdot10^{-2}$	-0.1299
1.5000	$2.3270\cdot10^{-2}$	$-1.6240\cdot10^{-3}$	$-2.2050\cdot10^{-2}$	-0.1622
1.5600	$2.6240\cdot10^{-2}$	$1.5800\cdot10^{-3}$	$-2.7470\cdot10^{-2}$	-0.1512
1.6600	$1.0280\cdot10^{-4}$	$-3.1860\cdot10^{-3}$	$-3.2350\cdot10^{-3}$	$-3.328\cdot10^{-3}$

As follows from the numerical simulation results, at $\hat{\omega}$=1.38070, almost periodic oscillations are observed in the dynamic system. The Poincaré sections of these movements are shown in Fig. 4. In these and subsequent figures, 4000 points will be shown in Poincaré sections. Fig. 4, a shows the section of an invariant torus. With an increase in the frequency of the disturbing action, the system exhibits a synchronization phenomenon on the invariant torus, that is, on this torus, in the phase space, there are high-order subharmonic oscillations. Fig. 4, b shows Poincaré sections of subharmonic oscillations of the 17th order. In this case, the maximum characteristic index is negative (Table 2). With a further increase in the frequency of the disturbing effect, chaotic oscillations are observed. The formation of chaotic oscillations after the synchronization on the invariant torus is called the order-chaos transition, which is described in monograph [9]. The Poincaré sections of

chaotic oscillations at $\hat{\omega}=1.4525$; $\hat{\omega}=1.50018$; $\hat{\omega}=1.66095$ are shown in Figs. 4, c, d, and e. The results of the calculation of the spectrum of Lyapunov characteristic indicators of such oscillations are shown in Table 2. As follows from this table, the maximum characteristic indicators are positive, which indicates the chaotic nature of oscillations. Fig. 5 shows the spectral densities of chaotic oscillations at $\hat{\omega}=1.50018$. As follows from the calculation results, the spectral densities contain three delta amplitudes. A continuous spectrum is observed near one of these amplitudes (majorant), which indicates the chaotic nature of steady-state oscillations.

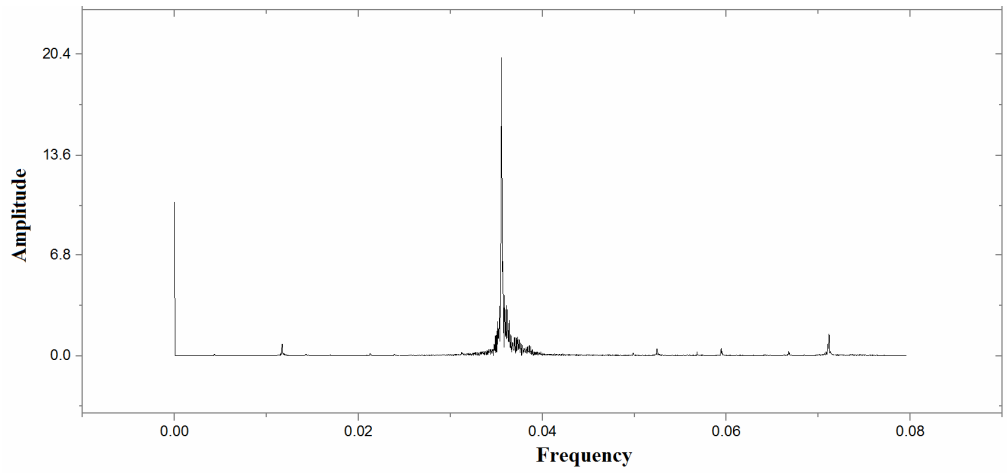

Fig.5. Spectral density of chaotic oscillations at $\hat{\omega}=1.50018$

Conclusions

A model of forced non-linear oscillations of kinematically excited flat shells during geometrically non-linear deformation is obtained. In this paper, a non-linear dynamic system with three degrees of freedom is obtained using the method of given forms. The system describes the second fundamental resonance of forced oscillations. In the area of the main second resonance, saddle-node bifurcations, period- doubling bifurcations, and Neimark-Sacker bifurcations are observed, which lead to the formation of almost periodic and chaotic oscillations. The almost periodic and chaotic oscillations observed in the region of the second main resonance are investigated. An order-chaos transition has been detected with a quasi-static change in the frequency of the disturbing action.

References

1. Avramov, K. V. & Mikhlin, Yu. V. (2015). *Nelineynaya dinamika uprugikh sistem: v 2-kh t. T. 2: Prilozheniya* [Non-linear dynamics of elastic systems: in 2 volumes. Vol. 2: Applications]. Moscow: Institute for Computer Research, 700 p. (in Russian).
2. Amabili, M. & Paidoussis, M. P. (2003). Review of studies on geometrically nonlinear vibrations and dynamics of circular cylindrical shells and panels, with and without fluid structure interaction. *Applied Mechanics Reviews*, vol. 56, iss. 4, pp. 349–381. https://doi.org/10.1115/1.1565084
3. Amabili, M. (2008). Nonlinear vibrations and stability of shells and plates. Cambridge: Cambridge University Press, 374 p. https://doi.org/10.1017/CBO9780511619694
4. Parker, T. S. & Chua, L. O. (1989). Practical numerical algorithms for chaotic systems. New York: Springer, 348 p. https://doi.org/10.1007/978-1-4612-3486-9
5. Meirovitch, L. (1986). Elements of vibration analysis. New York: McGraw-Hill Publishing Company, 495 p.
6. Awrejcewicz, J., Kurpa, L., & Osetrov, A. (2001). Investigation of the stress-strain state of the laminated shallow shells by R-functions method combined with spline-approximation. *Journal of Applied Mathematics and Mechanics*, vol. 91, iss. 6, pp. 458–467. https://doi.org/10.1002/zamm.201000164
7. Hollig, K., Reif, U., & Wipper, J. (2001). Weighted extended B-spline approximation of Dirichlet problems. *SIAM Journal on Numerical Analysis*, vol. 39, iss. 2, pp. 442–462. https://doi.org/10.1137/S0036142900373208
8. Cheshko, K. F., Polishchuk, O. F., & Avramov K. V. (2017). Eksperimentalnyy i chislennyy analiz svobodnykh kolebaniy pologoy obolochki [Experimental and numerical analysis of free shallow shell oscillations]. *Vestn. NTU «KhPI». Ser. Dinamika i prochnost mashin – Bulletin of NTU "KhPI". Series: Dynamics and Strength of Machines*, iss. 40 (1262), pp. 81–85 (in Russian). https://doi.org/10.20998/2078-9130.2017.40.119720

9. Avramov, K. V. & Mikhlin, Yu. V. (2015). *Nelineynaya dinamika uprugikh sistem: v 2-kh t. T. 1: Modeli, metody, yavleniya* [[Non-linear dynamics of elastic systems: in 2 volumes. Vol. 1: Models, methods, phenomena]. Moscow: Institute for Computer Research, 716 p. (in Russian).

Received 14 March 2019

Хаотичні коливання кінематично збуреної пологої оболонки при геометрично нелінійному деформуванні

К. В. Аврамов, К. Ф. Чешко, О. Ф. Поліщук

Інститут проблем машинобудування ім. А. М. Підгорного НАН України,
61046, Україна, м. Харків, вул. Пожарського, 2/10

Досліджуються вимушені коливання консольної пологої оболонки постійної кривизни. Ці рухи збуджуються кінематичним періодичним рухом защемлення. Для опису геометрично нелінійного деформування використовується нелінійна теорія оболонок Донелла. Для побудови нелінійної динамічної системи зі скінченним числом ступенів свободи застосовується метод заданих форм. Оскільки власні частоти поздовжніх і крутильних коливань значно вище згинальних, то інерційні сили в поздовжньому і крутильному напрямах не враховуються. Тому узагальнені координати поздовжніх і крутильних коливань виражаються через згинальні. Отже, отримана нелінійна динамічна система щодо згинальних узагальнених координат. Для розрахунку власних форм лінійних коливань, за якими розкладається нелінійна динамічна задача, використовується метод Релея-Рітца. Тоді задовольняються лише кінематичні граничні умови. За збіжності розв'язку силові граничні умови виконуються автоматично. Для дослідження збіжності власних частот проводилися розрахунки з різним числом базисних функцій. Як базисні функції використані B-сплайни. Проведено порівняння з експериментальними даними аналізу власних частот, опублікованими авторами раніше. Для числового аналізу нелінійних періодичних коливань розв'язана двоточкова крайова задача для звичайних диференціальних рівнянь методом пристрілки. Стійкість періодичних рухів і їх біфуркації оцінено за величинами мультиплікаторів. Для дослідження біфуркацій періодичних коливань застосовано метод продовження розв'язку по параметру. В області основного резонансу виявлено сідло-вузлові біфуркації, біфуркації подвоєння періоду та біфуркації Неймарка-Сакера. Для дослідження сталих майже періодичних і хаотичних коливань розраховано перетини Пуанкаре, спектри характеристичних показників Ляпунова і спектральні щільності. Як перетини Пуанкаре використано стробоскопічний фазовий портрет. Досліджено властивості сталих коливань за квазістатичної зміни частоти збуджуючої дії.

Ключові слова: *нелінійні періодичні коливання пологої оболонки, стійкість коливань, майже періодичні коливання, хаотичні коливання.*

Література

1. Аврамов К. В., Михлин Ю. В. Нелинейная динамика упругих систем: в 2-х т. Т. 2: Приложения. М.: Инт компьютер. исследований, 2015. 700 с.
2. Amabili M., Paıdoussis M. P. Review of studies on geometrically nonlinear vibrations and dynamics of circular cylindrical shells and panels, with and without fluid structure interaction. *Appl. Mech. Reviews*. 2003. Vol. 56. Iss. 4. P. 349–381. https://doi.org/10.1115/1.1565084
3. Amabili M. Nonlinear vibrations and stability of shells and plates. Cambridge: Cambridge University Press, 2008. 374 p. https://doi.org/10.1017/CBO9780511619694
4. Parker T. S., Chua L. O. Practical Numerical Algorithms for Chaotic Systems. New York: Springer, 1989. 348 p. https://doi.org/10.1007/978-1-4612-3486-9
5. Meirovitch L. Elements of vibration analysis. New York: McGraw-Hill Publishing Company, 1986. 495 p.
6. Awrejcewicz J., Kurpa L., Osetrov A. Investigation of the stress-strain state of the laminated shallow shells by R-functions method combined with spline-approximation. *J. Appl. Math. and Mech*. 2001. Vol. 6. P. 458–467. https://doi.org/10.1002/zamm.201000164
7. Hollig K., Reif U., Wipper J. Weighted extended B-spline approximation of Dirichlet problems. *J. on Numerical Analysis*. 2001. Vol. 39. No. 2. P. 442–462. https://doi.org/10.1137/S0036142900373208
8. Чешко К. Ф., Полищук О. Ф., Аврамов К. В. Экспериментальный и численный анализ свободных колебаний пологой оболочки. *Вісн. НТУ «ХПІ»*. 2017. № 40. С. 81–85. https://doi.org/10.20998/2078-9130.2017.40.119720
9. Аврамов К. В., Михлин Ю. В. Нелинейная динамика упругих систем: в 2-х т. Т. 1. Модели, методы, явления. М.: Ин-т компьютер. исследований, 2015. 716 с.